Magnetic Ordering in the Ammoniated Fulleride $(ND_3)K_3C_{60}$

Kosmas Prassides,*,† Serena Margadonna,† Denis Arcon,† Alexandros Lappas,† Hideo Shimoda,‡ and Yoshihiro Iwasa‡

School of Chemistry, Physics and Environmental Science University of Sussex, Brighton BN1 9QJ, U.K. Japan Advanced Institute of Science and Technology Tatsunokuchi, Ishikawa 923-1292, Japan

Received August 13, 1999

Intercalation of C_{60} with alkali metals leads to superconducting compositions A_3C_{60} (A = alkali metal) with critical temperatures as high as 33 K,[1] surpassed only by the high-T_c superconducting cuprates. It is well established that T_c increases monotonically with increasing interfullerene separation, *d*, as the density of states at the Fermi level, $N(\epsilon_F)$ increases.[2] Of paramount importance is the search for new materials with larger lattice parameters in order to establish whether T_c can be driven to higher values or the anticipated band narrowing will lead to electron localization and a transition to a Mott insulator.[3,4] Ammoniation has proven an excellent method to achieve large expansions of the fulleride unit cells, as neutral NH_3 molecules coordinate to the alkali ions, leading to large effective radii for the $(NH_3)_xA^+$ species. Successful ammoniation of Na_2CsC_{60} (T_c= 12 K) affords $(NH_3)_4$-Na_2CsC_{60} whose T_c increases to 29.6 K.[5] On the other hand, reaction of K_3C_{60} with NH_3 leads to orthorhombic $(NH_3)K_3C_{60}$ which is nonsuperconducting; however, application of a pressure >1 GPa leads to recovery of superconductivity with T_c= 28 K.[6] Structural characterization has identified a phase transition below 150 K, driven by the antiferroelectric ordering of the K^+-NH_3 pairs residing in the octahedral sites,[7] while the orientational dynamics of the C_{60}^{3-} ions are consistent with the existence of a weaker and more anisotropic potential than that encountered in the parent K_3C_{60}.[8] ESR and ^{13}C NMR measurements have shown that $(NH_3)K_3C_{60}$ is a narrow band metal which exhibits a transition to an insulating ground state at 40 K.[9]

Thus $(NH_3)K_3C_{60}$ is a key compound whose study is crucial for the understanding of the suppression of superconductivity at large interfullerene spacings. However, the nature of the low-temperature state appeared controversial as the experimental results were unable to distinguish between a magnetic (antiferromagnetic, spin-density wave) or a nonmagnetic (charge-density wave) ground state. In this contribution, we address the problem of the existence of nonzero internal local magnetic fields at low temperature in the perdeuterated analogue, $(ND_3)K_3C_{60}$ using 100% spin-polarized positive muons (μ^+) in the absence of external fields. These are implanted into the solid sample, and after they come to rest at an interstitial site, they act as highly sensitive microscopic local magnetic probes. In the presence of local magnetic fields, $\langle B_\mu \rangle$, they will precess with a frequency, $\nu_\mu = (\gamma_\mu/2\pi)\langle B_\mu \rangle$, where $\gamma_\mu/2\pi$ = 13.55 kHz/G. In the absence of an applied external field, the appearance of a precession signals the onset of an ordering (ferromagnetic or antiferromagnetic) transition. ZF-μ^+SR spectroscopy has proven extremely powerful in the field of small-moment magnetism and in instances when magnetic order is of random, very short-range, spatially inhomogeneous, or incommensurate nature.[10] In $(ND_3)K_3C_{60}$, we observe a heavily damped oscillating signal which provides unambiguous proof of antiferromagnetic long-range order below $T_N \approx 37$ K. The strong relaxation found in ZF is the signature of spatial disorder and inhomogeneity effects. In addition, the precession frequency varies with temperature on approaching T_N in the manner expected for a three-dimensional Heisenberg exchange model. These results provide clear evidence that the low-temperature state in ammoniated K_3C_{60} is that of an antiferromagnetic Mott insulator.

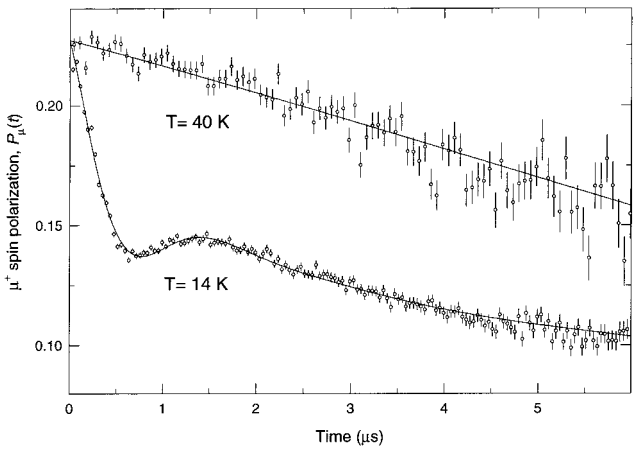

Figure 1. Evolution of the zero-field (ZF) μ^+ spin polarization, $P_\mu(t)$ at 14 and 40 K for $(ND_3)K_3C_{60}$. The solid lines through the data at 14 and 40 K are fits to the functions described in the text.

Figure 1 shows the ZF time-dependent μ^+SR spectra of (ND_3)-K_3C_{60} at 14 and 40 K. No oscillating signal is seen at 40 K and above. The spectra at high temperatures (40−100 K) were best-fitted by the double-relaxation function: $P_\mu(t) = A\ \exp(-\lambda t)$ $\exp(-{}^1/_2\sigma^2t^2)$, where *A* is the magnitude of the asymmetry, and λ and σ are Lorentzian and Gaussian relaxation rates, respectively. The Gaussian term with a temperature-independent relaxation rate, $\sigma \approx 0.07\ \mu s^{-1}$ is characteristic of the presence of weak static nuclear dipole moments. This muon relaxation arises principally from the deuterium nuclear moments, which appear frozen into a disordered spin configuration, producing a distribution of local fields with a width, $\langle \Delta B^2 \rangle^{1/2} \approx 2.4$ G. In addition, the μ^+ spin is relaxed by the rapidly fuctuating electron spins, which give rise to the Lorentzian component with $\lambda = 0.030(2)\ \mu s^{-1}$ at 100 K. Cooling-down leads to a slowing-down of the electron spin dynamics within the paramagnetic domains with λ approaching $0.046(1)\ \mu s^{-1}$ at 40 K.

Below 40 K (Figure 1), the shape of the μ^+SR spectra changes, as a short-lived component, whose depolarization gradually increases with decreasing temperature, appears. In fitting the data, we employ a strongly damped oscillating polarization signal superimposed on a slowly relaxing component: $P_\mu(t) = A_1$ $[{}^1/_3\exp(-{}^1/_2\sigma_1{}^2t^2) + {}^2/_3\exp(-\lambda_1 t)\ \cos(2\pi\nu_\mu t + \phi)] + A_2$ $\exp(-{}^1/_2\sigma_2{}^2t^2)$. A_1 and A_2 are amplitudes reflecting the fractions

† University of Sussex.
‡ Japan Advanced Institute of Science and Technology.

(1) Tanigaki, K.; Ebbesen, T. W.; Saito, S.; Mizuki, J.; Tsai, J. S.; Kubo, Y.; Kuroshima, S. *Nature* **1991**, *352*, 222.
(2) Fleming, R. M.; Ramirez, A. P.; Rosseinsky, M. J.; Murphy, D. W.; Haddon, R. C.; Zahurak, S. M.; Makhija, A. V. *Nature* **1991**, *352*, 787.
(3) Tanigaki, K.; Prassides, K. *J. Mater. Chem.* **1995**, *5*, 1515. Prassides, K. *Curr. Opin. Solid State Mater. Sci.* **1997**, *2*, 433. Rosseinsky, M. J. *Chem. Mater.* **1998**, *10*, 2665.
(4) Gunnarsson, O. *Rev. Modern Phys.* **1997**, *69*, 575.
(5) Zhou, O.; Fleming, R. M.; Murphy, D. W.; Rosseinsky, M. J.; Ramirez, A. P.; van Dover: R. B.; Haddon, R. C. *Nature* **1993**, *362*, 433.
(6) (a) Rosseinsky, M. J.; Murphy, D. W.; Fleming, R. M.; Zhou, O. *Nature* **1993**, *364*, 425. (b) Zhou, O.; Palstra, T. T. M.; Iwasa, Y.; Fleming, R. M.; Hebard, A. F.; Sulewski, P. E. *Phys. Rev. B* **1995**, *52*, 483.
(7) Ishii, K.; Watanuki, T.; Fujiwara, A.; Suemats, H.; Iwasa, Y.; Shimoda, H.; Mitani, T.; Nakao, H.; Fujii, Y.; Murakami, Y.; Kawada, H. *Phys. Rev. B* **1999**, *59*, 3956.
(8) Margadonna, S.; Prassides, K.; Neumann, D. A.; Shimoda, H.; Iwasa, Y. *Phys. Rev. B* **1999**, *59*, 943.
(9) Iwasa, Y.; Shimoda, H.; Palstra, T. T. M.; Maniwa, Y.; Zhou, O.; Mitani, T. *Phys. Rev. B* **1996**, *53*, R8836; Allen, K. M.; Heyes, S. J.; Rosseinsky, M. J. *J. Mater. Chem.* **1996**, *6*, 1445. Simon, F.; Janossy, A.; Iwasa, Y.; Shimoda, H.; Baumgartner, G.; Forro, L. In *Electronic Properties of Novel Materials*; Kuzmany, H., Fink, J., Mehring, M., Roth, S., Eds.; AIP Conference Proceedings 442. Woodbury, NY, 1998; p 296.
(10) Schenck, A. In *Frontiers in Solid State Science*; Gupta, L. C., Multani, M. S., Eds.; World Scientific: Singapore, 1993; Vol. II.

10.1021/ja992931k CCC: $18.00
Published on Web 11/19/1999

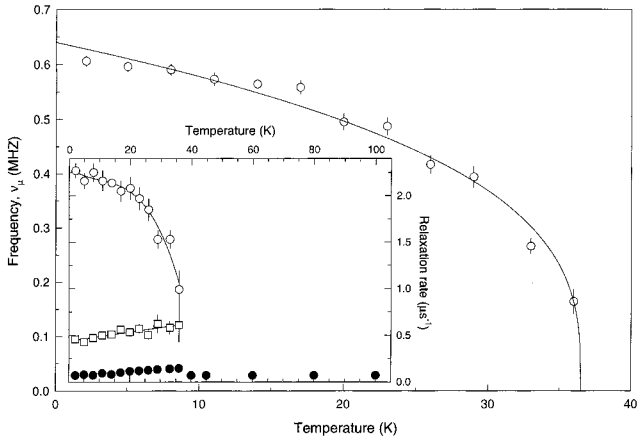

Figure 2. Temperature dependence of the muon precession frequency, ν_μ (○) in $(ND_3)K_3C_{60}$; the solid line is a fit of the data to the function described in the text. The inset shows the depolarization rates of the magnetically ordered, λ_1 (○) and σ_1 (□), and paramagnetic, σ_2 (●) components in $(ND_3)K_3C_{60}$; the solid lines through the points represent guides to the eye.

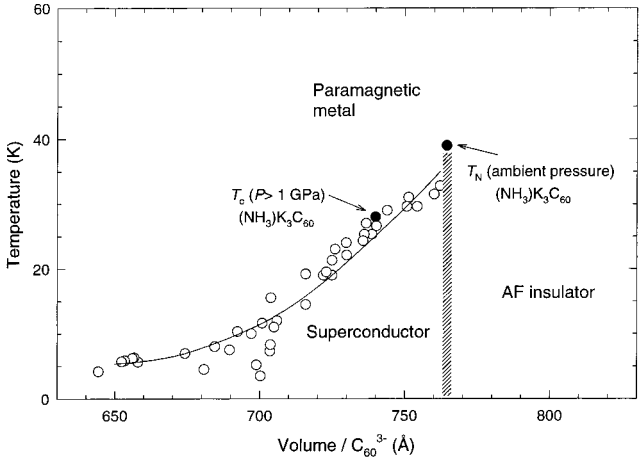

Figure 3. Schematic electronic phase diagram of C_{60}^{3-} compounds, showing the approximate location of the metal (superconductor)−insulator phase boundary. The open symbols are literature values of T_c for a variety of superconducting fullerides, while the solid symbols mark T_N (ambient pressure) and T_c (>1 GPa) of $(ND_3)K_3C_{60}$.

of the muons contributing to the two components, $\nu_\mu = \omega_\mu/2\pi$ is the μ^+ Larmor precession frequency and ϕ its phase, and λ_1, σ_1, and σ_2 are relaxation rates associated with the two components. The physical origin of the first term lies with the fact that on average, for a completely random distribution of the directions of the internal field in a powder sample, one-third of all muons experience an internal field along their initial spin direction, and consequently, they will not precess, giving rise to the $\exp(-{}^1/_2\sigma_1{}^2t^2)$ term; σ_1 represents relaxation due to field components perpendicular to the μ^+ spin. On the other hand, λ_1 reflects relaxation due to both dynamic and static field inhomogeneities along the μ^+ spin direction. The observation of ν_μ in zero external field is clear evidence of coherent ordering of the electronic spins and indicates the onset of long-range antiferromagnetic order. The frequency, ν_μ is 0.564(4) MHz at 14 K, corresponding to a static local field at the muon site, $\langle B_\mu \rangle = 41.6(3)$ G. In addition, the depolarization rate, λ_1 has a value of 2.14(4) μs^{-1} at 14 K, implying a distribution of local fields with a width $\langle \Delta B^2 \rangle^{1/2} = 25.1(4)$ G, only smaller than $\langle B_\mu \rangle$ by a factor of 1.7. The muons thus experience a local field with large spatial inhomogeneities, which may be due to a number of physical reasons, including orientational disorder effects of the fullerene molecules.

Figure 2 shows the variation of ν_μ with temperature down to 2 K. Its behavior is described by the equation: $\nu_\mu = \nu_0[1-(T/T_N)]^\beta$, with $\nu_0 = 0.64(1)$ MHz, $T_N = 36.5(3)$ K, and $\beta = 0.32(3)$. The critical exponent, β is close to the value expected for a conventional 3D Heisenberg antiferromagnet. As the μ^+ site is not known for a powder sample, a value of the magnetic moment cannot be extracted directly. However, we note that ν_0 is 1.4 times smaller than the frequency observed in the fullerene ferromagnet, $(TDAE)C_{60}$ (~0.92 MHz), in which the magnetic moment is 1 μ_B/molecule.[12] Assuming similar stopping sites for the two samples, we find $\mu(0\ K)$ is on the order of 0.7 μ_B/molecule. The depolarization rate, λ_1 also displays a similar temperature dependence to that of ν_μ, while the relaxation, σ_1 caused by field components perpendicular to the μ^+ spin weakly decreases with decreasing temperature to 0.46(2) μs^{-1} at 2 K (inset Figure 2). Data collected at 14 K in a 200 G longitudinal field reveal a complete recovery of the asymmetry. As the effect of applied longitudinal fields is to allow the depolarization due to dynamic or fluctuating moments to be decoupled from that due to static components, we conclude that the origin of the observed relaxation in zero field is of quasi-static nature. Finally, as the temperature is lowered, the volume fraction of the nonoscillating component (A_2) becomes smaller, while component A_1 which gives rise to the oscillating signal dominates at lower temperatures, as the volume fraction of the magnetically ordered domains grows at the expense of the paramagnetic ones. The data clearly imply an inhomogeneous form of magnetism even at 2 K with coexisting paramagnetic (~45%) and ordered static (~55%) local fields.

In conclusion, we have shown that $(ND_3)K_3C_{60}$ shows a transition below ~37 K to a long range ordered antiferromagnetic state, characterized by considerable spatially inhomogeneous effects. The importance of these results for the understanding of superconductivity in C_{60}^{3-} compounds is far reaching. The suppression of superconductivity and the metal−insulator transition are associated with effects of magnetic origin, providing an important analogy with the well-established phenomenology in high-T_c and organic superconductors. Thus the increased interfullerene separation in $(ND_3)K_3C_{60}$ has important consequences for the electronic properties of the material. The overlap between the molecules decreases substantially, leading to a reduced bandwidth, W and an increased (U/W) ratio, which for fixed-band filling drive the system to an antiferromagnetic Mott insulating state.[13] Then the recovery of superconductivity at pressures higher than 1 GPa ($T_c = 28$ K)[6b] should presumably be associated with the suppression of the magnetic transition. Figure 3 displays a schematic electronic phase diagram for C_{60}^{3-} compounds as a function of the volume per C_{60}^{3-} anion (or equivalently increasing (U/W) ratio). Future studies of the electronic properties of systems lying on either side of the metal (superconductor)−insulator phase boundary promise to lead to intriguing results.

Acknowledgment. We thank NEDO FCT, the British Council, the JSPS, and the Japanese Ministry of Education, Science, Sports, and Culture for financial support, the PSI for provision of muon beamtime, A. Amato and D. Herlach for help with the experiments, and A. Schenck and M. Pinkpank for useful discussions.
JA992931K

(11) The $(ND_3)K_3C_{60}$ sample used in the present work was prepared by reaction of single-phase K_3C_{60} powder with ND_3 gas, as described before.[8] Phase purity was confirmed by powder X-ray diffraction using a Siemens D5000 diffractometer. Zero-field (ZF) and longitudinal-field (LF 200 G) μ^+SR data were collected at the Paul Scherrer Institute (PSI), Villigen, Switzerland, with the general purpose spectrometer (GPS) using low-energy (surface) muons on the μ^+SR dedicated πM3 beamline on the PSI 600 MeV proton accelerator. The powder sample (194 mg) was sealed under argon in a silver sample holder, equipped with indium seals and Mylar windows, and placed inside a continuous-flow helium cryostat. Measurements were performed in the temperature range 2−100 K, with data collection (~15 million events) taking ~1 h per dataset, except for a 11-h high statistics (~150 million events) run at 14 K.

(12) Lappas, A.; Prassides, K.; Vavekis, K.; Arcon, D.; Blinc, R.; Cevc, P.; Amato, A.; Feyerherm, R.; Gygax, F. N.; Schenck, A. *Science* **1995**, *267*, 1799. Tokumoto, M.; Tsubaki, Y.; Pokhodnya, K.; Omerzu, A.; Uchida, T.; Mihailovic, D. *Synth. Met.* **1999**, *103*, 2316.

(13) Koch, E.; Gunnarsson, O.; Martin, R. M. *Phys. Rev. Lett.* **1999**, *83*, 620.